ACCOUNTS
of chemical research

# Non-Fullerene Electron Acceptors for Use in Organic Solar Cells

Christian B. Nielsen,*,[†] Sarah Holliday,[†] Hung-Yang Chen,[†] Samuel J. Cryer,[†] and Iain McCulloch[†,‡]

[†]Department of Chemistry and Centre for Plastic Electronics, Imperial College London, London SW7 2AZ, United Kingdom

[‡]Physical Sciences and Engineering Division, King Abdullah University of Science and Technology (KAUST), Thuwal 23955−6900, Saudi Arabia

CONSPECTUS: The active layer in a solution processed organic photovoltaic device comprises a light absorbing electron donor semiconductor, typically a polymer, and an electron accepting fullerene acceptor. Although there has been huge effort targeted to optimize the absorbing, energetic, and transport properties of the donor material, fullerenes remain as the exclusive electron acceptor in all high performance devices. Very recently, some new non-fullerene acceptors have been demonstrated to outperform fullerenes in comparative devices. This Account describes this progress, discussing molecular design considerations and the structure−property relationships that are emerging.

The motivation to replace fullerene acceptors stems from their synthetic inflexibility, leading to constraints in manipulating frontier energy levels, as well as poor absorption in the solar spectrum range, and an inherent tendency to undergo postfabrication crystallization, resulting in device instability. New acceptors have to address these limitations, providing tunable absorption with high extinction coefficients, thus contributing to device photocurrent. The ability to vary and optimize the lowest unoccupied molecular orbital (LUMO) energy level for a specific donor polymer is also an important requirement, ensuring minimal energy loss on electron transfer and as high an internal voltage as possible. Initially perylene diimide acceptors were evaluated as promising acceptor materials. These electron deficient aromatic molecules can exhibit good electron transport, facilitated by close packed herringbone crystal motifs, and their energy levels can be synthetically tuned. The principal drawback of this class of materials, their tendency to crystallize on too large a length scale for an optimal heterojunction nanostructure, has been shown to be overcome through introduction of conformation twisting through steric effects. This has been primarily achieved by coupling two units together, forming dimers with a large intramolecular twist, which suppresses both nucleation and crystal growth. The generic design concept of rotationally symmetrical aromatic small molecules with extended π orbital delocalization, including polyaromatic hydrocarbons, phthalocyanines, etc., has also provided some excellent small molecule acceptors. In most cases, additional electron withdrawing functionality, such as imide or ester groups, can be incorporated to stabilize the LUMO and improve properties. New calamitic acceptors have been developed, where molecular orbital hybridization of electron rich and poor segments can be judiciously employed to precisely control energy levels. Conformation and intermolecular associations can be controlled by peripheral functionalization leading to optimization of crystallization length scales. In particular, the use of rhodanine end groups, coupled electronically through short bridged aromatic chains, has been a successful strategy, with promising device efficiencies attributed to high lying LUMO energy levels and subsequently large open circuit voltages.
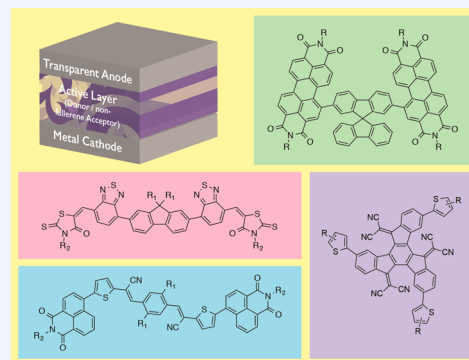
■ INTRODUCTION

In the field of organic photovoltaics (OPV), there is a growing interest in developing new electron acceptor materials in addition to the prevalent fullerene-based acceptors such as phenyl-C_{61}-butyric acid methyl ester ($PC_{61}BM$) and phenyl-C_{71}-butyric acid methyl ester ($PC_{71}BM$). These fullerene acceptors were derived from the parent C_{60} and C_{70} fullerenes to improve the solubility and processability, in particular for bulk heterojunction (BHJ) solar cells. Their dominance in the OPV research landscape stems from advantageous properties including (i) the ability to accept and transport electrons in three dimensions thanks to a LUMO that is delocalized over the whole surface of the molecule, (ii) high electron mobilities, (iii) multiple reversible electrochemical reductions, and (iv) the ability to aggregate in bulk heterojunctions to form both pure and mixed domains of the appropriate length scale for charge separation. Nevertheless, fullerene-based acceptors have some significant limitations including (i) weak absorption in the abundant region of the incident solar spectrum, which limits their ability to harvest photocurrent, (ii) limited tunability in terms of spectral absorption, (iii) high synthetic costs, especially for the high performing C_{70} derivative, and (iv) morphological instability due to fullerene diffusion and aggregation in the thin film over time.

Much research has been focused on developing appropriate and efficient donor materials optimized specifically for these fullerenes and also accommodating their limitations in terms of absorption profile and electronic properties. The development of new donor materials using this approach has undoubtedly
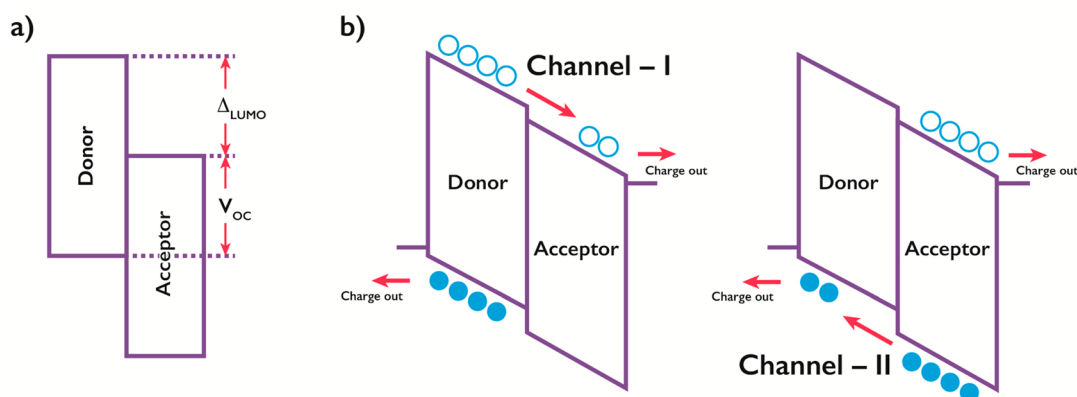
Figure 1. Donor−acceptor band diagrams showing energetic relationships (a) and mechanisms for photocurrent generation from p-type (channel I) and n-type (channel II) excitation (b).

advanced the OPV field significantly with single-junction devices now exceeding 10% power conversion efficiency (PCE).[1] However, the fine-tuning of molecular and electronic properties of the electron donor to exactly fulfill the requirements dictated by the fullerenes is a rigid and suboptimal design strategy. A more modular and dynamic approach to further enhance OPV device performance focuses on the development of new non-fullerene acceptors (NFAs) to be used in conjunction with the vast number of small molecule and polymeric donor materials that have been developed over the past decade.

New NFAs should obviously retain the advantageous properties of the fullerenes, such as efficient charge transfer with a low possibility of back transfer and good blend morphology with the donor material. They should also display greater ease of synthesis, improved solubility and processability from environmentally friendlier solvents, and increased optical absorptivity and introduce a structural flexibility that allows for favorable matching of frontier energy levels of donor and acceptor materials (Figure 1a).

NFAs that are slightly weaker electron acceptors than fullerenes are likely to work well with wide band gap donors such as poly(3-hexylthiophene-2,5-diyl) (P3HT) due to the diminished LUMO−LUMO offset (Δ_{LUMO}) affording a higher open-circuit voltage (V_{OC}). On the other hand, the availability of stronger electron acceptors than fullerenes is important when considering narrow band gap donors, which often perform poorly with fullerene acceptors due to an insufficient LUMO−LUMO offset. The low optical absorptivity of fullerenes means that the dominant mechanism for photo-current generation in fullerene based OPV devices is through p-type excitation and subsequent electron transfer (channel I, Figure 1b). The prospects of much stronger absorbing NFAs open up options for additional photocurrent generation through n-type excitation followed by hole transfer from the NFA to the electron donor material (channel II).[2,3] The coexistence of these two mechanisms for photocurrent generation in NFA based OPV devices emphasizes the importance of spectral complementarity and judicious matching of not only the LUMO energy levels for efficient electron transfer but also the highest occupied molecular orbital (HOMO) energy levels for hole transfer.

In this Account, we highlight and discuss some of the important classes of materials that have shown promise as alternative electron acceptor materials in organic solar cells. We relate important molecular structural characteristics to OPV device properties and discuss synthetic design criteria to aid the continued advancement of this important area of OPV research.

■ PERYLENE DIIMIDE AND FUSED AROMATIC RING ACCEPTORS

The most widely investigated NFA molecules to date have been based on the perylene diimide (PDI) core unit, which has been shown to possess many desirable design features for OPV electron acceptors, such as high electron mobility and high electron affinity (EA; ca. 3.9 eV for the unmodified PDI, which is similar to widely used fullerene acceptors).[4] In solution-processed BHJ OPVs, however, the progress has often been limited due to the strong $\pi−\pi$ stacking tendency of PDIs to form micrometer-sized crystallites, which are too large, preventing a sufficiently large donor−acceptor interfacial area for efficient exciton splitting. An attractive feature of PDI molecules, conversely, is that the $\pi−\pi$ stacking can generate crystal motifs suitable for charge transport. Hence, avoiding the formation of large PDI domains without sacrificing the charge transport ability of PDI is a molecular design conundrum for PDI-based NFAs in recent years.

Three functionalization positions (see Figure 2) have been exploited for the design of PDI-based NFAs for solution-processed BHJ OPVs. Initially, PDI molecules with only imide-functionalization were investigated. One strategy to disrupt the cofacial stacking in these molecules was the design of a PDI dimer (**1.1**, Figure 2) using hydrazine as a linker in the imide position, allowing twisting of the dimer and thus suppression of crystallinity.[5] An average domain size of about 10 nm was observed for the blend of PBDTTT-C-T/**1.1a** (1:1), which resulted in a PCE of 3.2% with a high J_{SC} of 9.0 mA/cm² (Table 1). Judicious optimization of both the acceptor and the polymer donor recently resulted in an improved PCE of 5.45% for **1.1b** (Table 1).[6] With a better understanding of the crystallite size on the influence of photovoltaic performance, more attention was focused on designing PDI NFAs with bay substituents (positions 1, 6, 7, and 12) due to synthetic accessibility and demonstrated success in minimizing PDI aggregation. Twisted PDI dimer structures have continued to be exploited as an efficient strategy for their use in BHJ OPVs. For example, a single bay-linked PDI dimer (**1.2**)[7] with about a 70° angle between two PDI units demonstrated good OPV performance arising from its flexibly twisted structure. BHJ OPV devices based on the **1.2** acceptor and the (PBDTT-F-TT) polymer donor demonstrated a PCE up to 5.90% by using an inverted cell structure with a fullerene self-assembled monolayer (C_{60}-
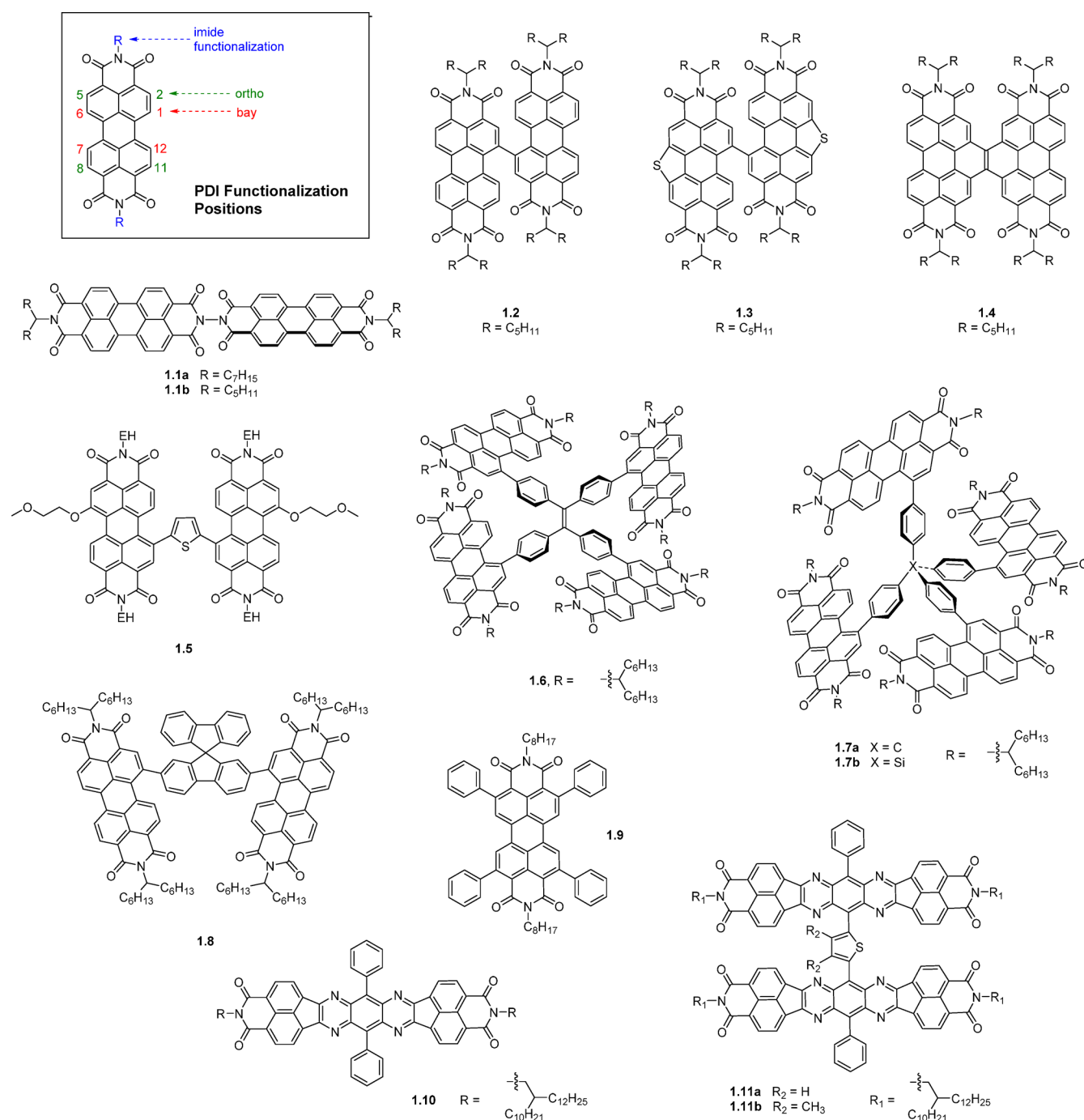
Figure 2. Chemical structures of PDI-based and fused aromatic ring electron acceptors.

SAM) on ZnO.[8] A closely related PDI dimer (**1.3**) with sulfur bridges in the bay positions had a more twisted molecular configuration, a slightly lower electron affinity, and a blue-shifted absorption profile providing better spectral complementarity with narrow band gap donor polymers.[9] Consequently, a high PCE of 7.16% was achieved with the PDBT-T1 donor polymer owing to a high V_{OC}, as well as good J_{SC} and FF values. Another PDI dimer with a two-carbon bridge (**1.4**), which has a nonplanar conformation from the repulsion between the two C−Hs on inner bay positions, demonstrated an average PCE of 5.52% with PBDTT-TT donor polymer, which was increased to 6.05% with solvent additives.[10] Nonplanar PDI conformations can also be achieved by

inserting an aromatic bridge between the two PDI units. A thienyl-bridged PDI dimer, **1.5**, which has a dihedral angle of 50°−60° between the two PDI−thienyl planes, showed significant reduction of the aggregation compared with its monomeric counterpart in BHJ blends.[11] Compound **1.5** yielded small phase domains with a size of ~30 nm with a corresponding PCE of up to 4.03%, while its monomeric counterpart produced crystalline domains on the order of hundreds of nanometers with a PCE of only 0.13%. Further fine-tuning of the film-forming process by solvent additives and solvent vapor annealing also improved the PCE to 6.1%.[12] Other molecular bridges were also demonstrated to be useful for suppressing the formation of micrometer-sized PDI

Table 1. Photovoltaic Performance and Ionization Potential (IP) and Electron Affinity (EA) Values of PDI-Based and Fused Aromatic Ring Electron Acceptors

acceptor	EA (eV)	IP (eV)	donor	PCE (%)	V_{OC} (V)	J_{SC} (mA/cm^2)	FF	ref
1.1a	4.06	6.02	PBDTTT-C-T	3.20	0.77	9.00	0.46	5
1.1b	3.86	5.90	PBDT-TS1	5.45	0.80	12.85	0.53	6
1.2	4.04	6.13	PBDTT-F-TT	5.90	0.80	11.98	0.59	8
1.3	3.85	6.05	PDBT-T1	7.16	0.90	11.98	0.66	9
1.4	3.77	6.04	PTB7	5.21	0.79	10.90	0.60	10
			PBDTT-F-TT	6.05	0.80	13.30	0.57	
1.5	3.84	5.65	PBDTTT-C-T	6.08	0.84	12.83	0.56	12
1.6	3.72	5.77	PBDTT-F-TT	5.53	0.91	11.70	0.52	14
1.7a	3.75	6.00	PffBT4T-2DT	4.3	0.96	9.2	0.49	15
1.7b	3.75	6.01	PffBT4T-2DT	4.2	0.94	8.5	0.53	15
1.8	3.83	5.90	PffBT4T-2DT	6.30	0.98	10.70	0.57	17
1.9	4.01	6.02	PBTI3T	3.67	1.03	6.56	0.55	19
1.11a	3.80	5.80	PSEHTT	5.04	0.86	10.14	0.58	20
1.11b	3.66	5.82	PSEHTT	6.37	0.92	12.56	0.55	21

aggregates.[13] For example, a tetraphenylethylene core based PDI NFA (**1.6**) showing a small domain size of 20 nm when blended with polymer donor PBDTT-F-TT, demonstrated a PCE of up to 5.53%.[14] The high performance of this blend was attributed to not only the inhibition of forming large acceptor crystallites, but it was also proposed that there was a formation of a 3D charge-transporting network created from its unique 3D molecular structure, with corresponding improved electron mobility. Moreover, the BHJ OPV device with **1.6** showed a high V_{OC} of 0.91 V, which is significantly higher than that of a PC$_{61}$BM-based solar cell due to its more favorable electron affinity (3.72 eV) than that of PC$_{61}$BM. A similar approach using tetraphenylmethane and tetraphenylsilane (**1.7**) as the core was slightly less efficient affording PCEs of 4.3% and 4.2%, respectively, for **1.7a** and **1.7b**.[15] Another case that utilizes the spirobifluorene bridge, **1.8**,[16,17] also demonstrated an impressive V_{OC} as large as 0.98 V when blended with the polymer donor PffBT4T-2DT, due to its electron affinity of 3.83 eV. The electron transport ability of **1.8** is reasonably good among reported PDI-based acceptors, which achieved a high fill factor (FF) of 65% in a P3HT/**1.8**-based solar cell; however, only moderate PCE of 2.35% was obtained due to the low V_{OC} of 0.61 V.[16] When blended with the low band gap polymer donor PffBT4T-2DT, the absorption of PffBT4T-2DT is complementary to **1.8**, resulting different regions of coverage for the solar spectrum. This selection of polymer donor/nonfullerene acceptor pair achieved a high PCE of 6.30% without any solvent additives and interlayers. An alternative strategy to control the molecular stacking of PDI molecules was to promote a slip-stacked crystalline motif, which can suppress face-to-face π–π stacking and, moreover, reduce the formation of excimers (which act as traps for excitation energy). Slip-stacked PDI dimers have been shown to exhibit an order of magnitude slower excimer formation than cofacial PDI dimer counterparts.[18] For example, PDI NFA **1.9** with four phenyl groups substituted in *ortho*-positions (2, 5, 8, and 11) was found to have a slip-stacked packing structure.[19] When blended with the PBTI3T, small crystalline acceptor grains (∼2−5 nm) resulted, with higher yields of long-lived charge separated species, resulting in a higher PCE of up to 3.67%.

Heterocyclic diimides, tetraazabenzodifluoranthenes (BFIs), were synthesized by the fusion of the heterocyclic ring tetraazaanthracene and two naphthalene imide units.[22] This large ladder-type molecule forms a slipped face-to-face π−π

stacking in its crystal structure, and the displacement between two neighboring BFI molecules is less than one-sixth of the length of the molecule, which is relatively smaller than that of PDI. Linking two BFI units in the central tetraazaanthracene position with thiophene promotes a nonplanar 3D molecule, **1.11a**, which showed an improved performance over the monomeric analogue (**1.10**) (and PC$_{61}$BM) in blends with PSEHTT donor polymer, demonstrating a maximum PCE of 5.04% in inverted BHJ structures.[20] The enhanced charge photogeneration of **1.11a** was shown by time-resolved microwave conductivity (TRMC) studies, with a significantly higher transient photoconductivity maxima ($\Delta\sigma_{max}$) observed. The slightly lower EA of **1.11a** than PC$_{61}$BM also provides an improvement in the V_{OC} of the BHJ OPV device. Molecule **1.11b** was subsequently found to have a significantly improved PCE of 6.4% ascribed to more efficient molecular packing and improved isotropic charge transport due to a more twisted molecular conformation caused by steric interactions with the methyl groups.[21]

ROTATIONALLY SYMMETRIC MOLECULES

From a synthetic point of view, it is often desirable to design symmetrical molecules, and this strategy has frequently been manifested in the development of NFAs. With inspiration from the archetypal electron acceptor C$_{60}$, several electron accepting motifs with rotationally symmetric polycyclic aromatic cores comprising five- and six-membered rings have been developed for use in OPV devices. One example of this approach is the C$_5$-symmetric corannulene (Figure 3), where the aromatic core is a fragment of C$_{60}$ and therefore bears resemblance to C$_{60}$ with respect to electron affinity as well as molecular curvature.[23] Another example is the C$_3$-symmetric truxenone (Figure 3),

C$_{60}$
C$_2$-, C$_3$-, C$_5$-symmetry

corannulene
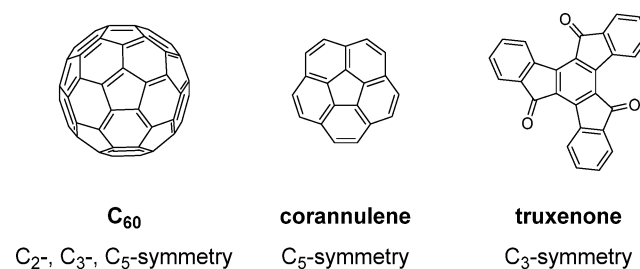C$_5$-symmetry

truxenone
C$_3$-symmetry

Figure 3. Examples of electron acceptor motifs derived from C$_{60}$.
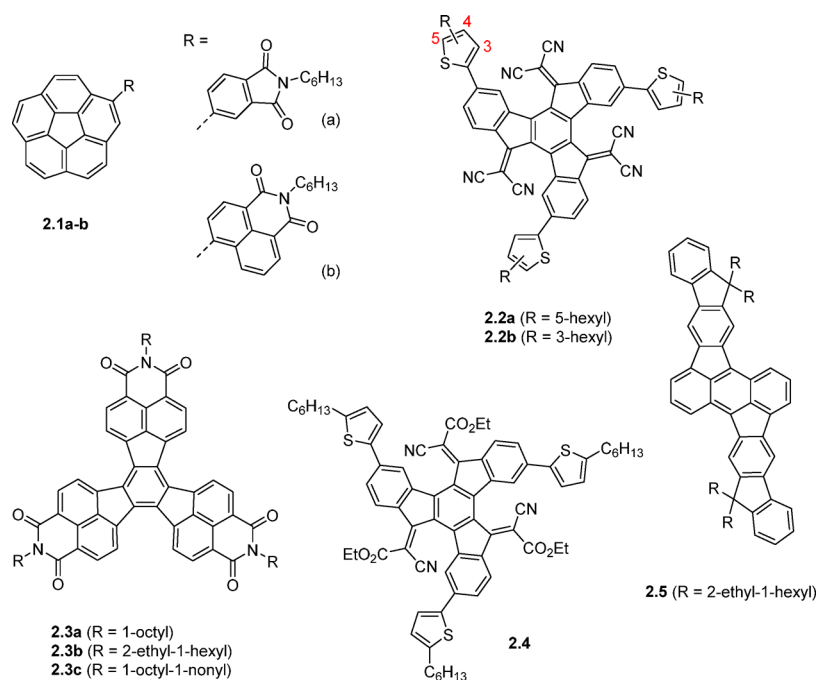
Figure 4. Electron acceptors based on rotationally symmetric aromatic cores.

Table 2. Photovoltaic Performance and Ionization Potential (IP) and Electron Affinity (EA) Values of Rotationally Symmetric Electron Acceptors

acceptor	EA (eV)	IP (eV)	donor	PCE (%)	V_{OC} (V)	J_{SC} (mA/cm^2)	FF	ref
2.1b	3.24	6.28	P3HT	1.03	0.82	2.75	0.46	27
2.2a	4.07	5.94	**2.6**	1.0	0.95	1.9	0.52	28
2.3c	3.61	5.81	P3HT	1.6			0.57	30
2.5	3.30	5.38	P3HT	3.05	1.22	4.29	0.58	32
2.6	3.6		6T	4.69	1.09	7.46	0.58	33
2.7	3.6		6T	6.02	0.94	12.04	0.54	33
2.8	3.61		**2.7**	6.86	1.04	10.1	0.67	35
2.9	3.95	5.7	**2.6**	4.0	0.95	7.8	0.54	36
2.10b	3.5	5.6	PTB7	3.51	0.94	7.8	0.48	37

which can be viewed as a planarized keto-functionalized C_{60} fragment.[24] This design strategy crucially relies on further structural functionalization to adjust the frontier energy levels and to create appropriately soluble materials that can be processed with electron donors to form phase separated BHJ blends with domain sizes comparable to the exciton diffusion length.

Despite the close resemblance to C_{60}, very few corannulene derivatives have been reported in the context of organic electronics.[25,26] Corannulenes **2.1a,b** (Figure 4) with a phthalimide and a naphthalimide substituent, respectively, were reported.[27] With electron affinities of 3.10 eV for **2.1a** and 3.24 eV for **2.1b**, these compounds are significantly weaker electron acceptors than, for example, $PC_{61}BM$. Compound **2.1b**, with the higher EA, was found to possess significantly higher electron mobility than **2.1a** and consequently performed reasonably well in a BHJ OPV device with P3HT as the donor material affording a high V_{OC} of 0.82 V and a PCE of 1.03% (Table 2). The authors found the imide substituents to be twisted relative to the corannulene core due to steric hindrance between aromatic protons, and semiempirical calculations indicated that the LUMO in both cases is predominantly localized on the peripheral substituent, which is also supported

by the fact that the electron affinities match closely the electron affinities of the phthalimide and naphthalimide moieties.

Truxenone derivatives **2.2** and **2.4**, in contrast, have their LUMOs widely distributed over the core of the molecule, and the electron affinities are controlled by the electron-withdrawing nature of the substituents on the vinylene group.[28,29] The dicyanovinylene motif in **2.2** results in an EA of approximately 4.1 eV, while the cyanoester adduct of **2.4** provides an EA of 3.9 eV. Compound **2.2a** outperforms $PC_{61}BM$ in a bilayer OPV structure with an evaporated subphthalocyanine donor material, giving a PCE of 1.0%, but this promising performance has yet to be demonstrated in a BHJ system. The Knoevenagel functionalization of truxenone, which converts the flat aromatic core to a bowl-shaped structure, is an effective means to control the EA and readily provides truxenone derivatives such as **2.2** with greater electron affinities than $PC_{61}BM$. While many NFAs are slightly weaker electron acceptors than $PC_{61}BM$ and primarily have been shown to work with wide band gap donors such as P3HT, the availability of stronger acceptors such as **2.2** is important when considering narrow band gap donors. Further investigation of truxenone derivative **2.4** indicated very low electron mobility, which could be one of the limiting factors for this class of materials.

The electron-deficient decacyclene-based triimide **2.3** was reported and initial studies afforded a PCE of 1.6% with compound **2.3c** in a BHJ solar cell with P3HT as the donor material.[30] In contrast, **2.3b** only afforded a PCE of 0.03% when tested under identical conditions, which highlights the important role of controlling the solubility, crystallinity, and BHJ blend morphology through alkyl-chain engineering. Further studies on **2.3c** have encouragingly indicated that this electron accepting material works reasonably well with a range of polymeric donor materials with band gaps varying from 1.8 to 2.0 eV and EAs from 3.3 to 3.7 eV.[31] PCEs range from 0.75% to 1.47% and V_{OC} values are in two cases significantly increased relative to the devices with $PC_{61}BM$ and $PC_{71}BM$. Compared with the conventional fullerene acceptors, all NFA devices presented in this study are limited by low fill factors and reduced J_{SC}-values, which the authors ascribe to suboptimal phase separation. The C_2-symmetric acceptor **2.5**, based on the C_{70} fragment rubicene, was demonstrated to have a high V_{OC} of 1.22 V and a PCE of 3.05% in a BHJ solar cell with P3HT as the donor material.[32]

Subphthalocyanines (SubPcs, Figure 5 and Table 2), and in particular boron SubPc chlorides, are another class of
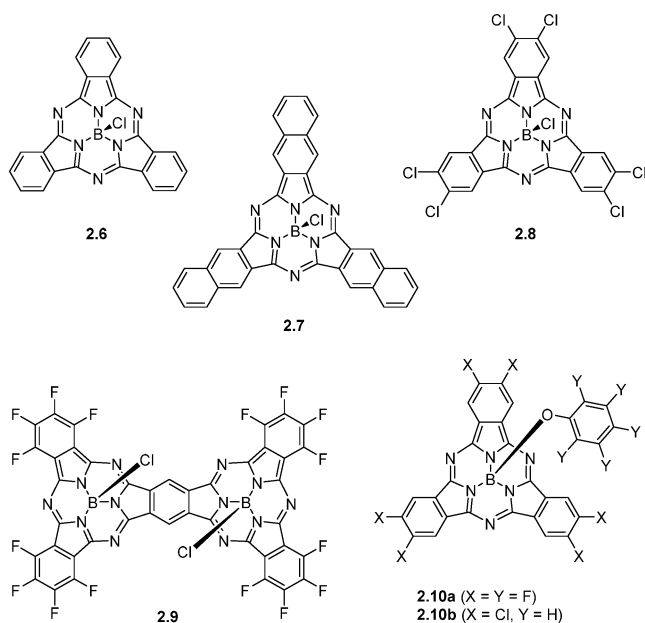

Figure 5. Electron acceptors based on rotationally symmetric subphthalocyanines.

rotationally symmetric molecules that have shown great promise in OPV applications. Bilayer devices using either **2.6** or **2.7** as the acceptor material with an α-sexithiophene donor afforded high PCEs of 4.69% and 6.02%, respectively.[33] Moreover, efficiencies as high as 8.40% were achieved with a three-layer device architecture employing both **2.6** and **2.7** due to a high V_{OC} of 0.96 V, a J_{SC} of 14.55 mA/cm², and a FF of 61%. The three photoactive materials have complementary optical absorption profiles and both internal (IQE) and external quantum efficiency (EQE) spectra importantly show efficient photocurrent generation by all three absorbing materials. Interestingly, **2.7** was also used as a donor material in conjunction with chlorinated electron acceptor **2.8**.[34] A planar heterojunction was again utilized, and with interlayer optimization, a PCE of 6.4% was achieved owing to a V_{OC} of

1.03 V, a J_{SC} of 9.0 mA/cm², and a FF of 71%. Compared with the corresponding device with C_{60} as the electron acceptor, an increased current with **2.8** was attributed to strong and complementary absorption profiles, while the greatly improved fill factor was explained by decreased recombination of either charge-transfer states or trapped charges. More recently, an improved PCE of 6.9% was reported for this system.[35] In a similar fashion, **2.9** was used as the electron acceptor with **2.6** as the donor to afford a bilayer OPV device with a PCE of 4.0%.[36] More recently, SubPc derivatives **2.10a,b** were employed in BHJ solar cells with three different donor polymers, MEH-PPV, P3HT, and PTB7.[37] Compounds **2.10a,b** were found to have 0.2 eV lower EA than PCBM. Despite the lower electron affinity, giving rise to a small energy offset on the order of 0.2 eV with donor polymer PTB7, a PCE of 3.5% was achieved with **2.10b**. Poorer device performances were observed with MEH-PPV (0.4% PCE) and P3HT (1.1% PCE), just as **2.10a** in all three cases underperformed relative to **2.10b** most likely due to a higher propensity for aggregation and crystallization. EQE spectra showed evidence of photocurrent generation from both electron and hole transfer (channels I and II), while main loss mechanisms were identified as limited exciton dissociation (due to small Δ_{LUMO}), high degree of trap-assisted recombination, and poor spectral matching with the solar spectrum.

■ CALAMITIC MOLECULES

Calamitic shaped small molecules, with discrete separation of electron rich and poor sections, have received attention recently as a promising class of NFAs, drawing on the symmetric monomer design template used in donor polymer synthesis. A conjugated push−pull structure can be achieved by combining electron rich and electron poor structural units, thereby reducing the optical bandgap via molecular orbital hybridization, which helps to extend the absorption, as well as offering control over the separation of the HOMO and LUMO electron density in the molecule in order to facilitate charge transfer. Convergent synthesis routes, whereby each unit is prepared separately before being combined together in the final structure, give synthetic flexibility, as well as benefiting final yields.

Figure 6 shows a typical, but not universal, structural template for high performance calamitic NFAs such as those
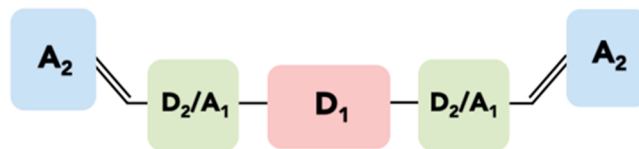

Figure 6. Schematic diagram of a typical calamitic NFA structure.

shown in Figure 7. This includes three different structural units: a central donor unit (D_1) that is flanked by a second donor or acceptor (D_2/A_1) unit and a terminal acceptor unit (A_2), often attached via a vinyl linkage. Using an electron rich moiety such as fluorene,[38−40] dibenzosilole,[41,42] indacenodithiophene,[43−45] and indacenodithieno[3,2-b]thiophene[46] as the central D_1 unit gives the advantage of solubility and crystallinity control through the alkyl chains that can be added to such moieties. It should be noted that there are examples of calamitic NFAs with electron deficient central units such as benzothiadiazole and its derivatives[2,47] or fluoranthene-fused imide,[48] but thus far,
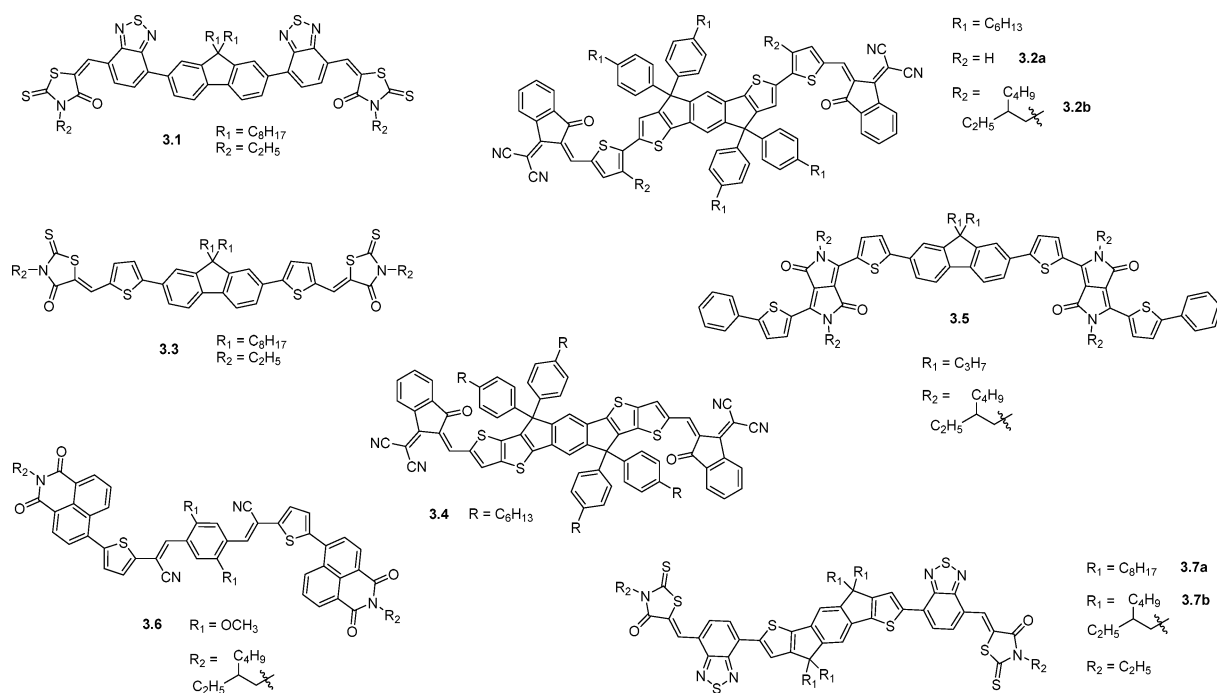
Figure 7. Calamitic-type electron acceptors with power conversion efficiencies >3%.

Table 3. Photovoltaic Performance and Ionization Potential (IP) and Electron Affinity (EA) Values of Calamitic-Type Electron Acceptors

acceptor	EA (eV)	IP (eV)	donor	PCE (%)	V_{OC} (V)	J_{SC} (mA/cm²)	FF	ref
3.1	3.57	5.70	P3HT	4.11	0.82	7.95	0.63	40
3.2a	3.25	5.11	PBDTTT-C-T	3.93	0.90	8.33	0.52	43
3.2b	3.82	5.42	PTB7-TH	6.31	0.97	13.55	0.48	44
3.3	3.53	5.58	P3HT	3.08	1.03	5.70	0.52	51
3.4	3.83	5.48	PTB7-TH	6.80	0.81	14.21	0.59	46
3.5	3.39	5.21	P3HT	3.17	1.18	5.35	0.50	39
3.6	3.66	5.75	p-DTS(FBTTh₂)₂	5.44	0.85	9.62	0.64	50
3.7a	3.88	5.45	P3HT	6.38	0.73	14.1	0.62	45
3.7b	3.90	5.57	P3HT	6.03	0.77	12.2	0.64	45

device performance from these materials has been lower relative to those with electron rich cores. This may be in part because typical electron deficient units like benzothiadiazole have no positions available for alkyl chains and therefore solubilizing groups must be located on the periphery of the molecule, making the LUMO less sterically accessible for electron transfer. In the case of polymer–fullerene systems, it is generally understood that the electron-deficient moieties on the polymer should be sterically accessible in order to facilitate "docking" with the fullerene.[49] In the same way, it is hypothesized that by locating bulky alkyl groups on the electron rich part of the NFA molecule, charge transfer may be improved by improved registry with the electron deficient parts of the polymer. Notable exceptions to this include **3.5** and **3.6** (Figure 7), which have alkylated diketopyrrolopyrrole and naphthalimide acceptors on the periphery, although it may be argued that these groups are large enough to not suffer from steric hindrance from their alkyl groups.

The D₂/A₁ flanking unit mainly serves the purpose of extending the conjugation and further tuning the molecule's energy levels. Typical donor units such as thiophene are often used here, but the molecules **3.1** and **3.7** (Figure 7) instead use the electron withdrawing benzothiadiazole unit in this position,

which helps to extend the LUMO to give this molecule a large and sterically exposed electron accepting component on the periphery. Device efficiencies up to 6.4% are achieved with this design, which are the highest efficiencies for P3HT based devices with calamitic NFAs, suggesting that this is an effective design strategy.[45]

Figure 7 and Table 3 show the structures and device performance parameters of calamitic NFAs giving power conversion efficiencies above 3%. Several important factors contribute to the performance of such materials. First, a large extinction coefficient in the acceptor is necessary to improve light absorption relative to fullerene-based devices. Most of the NFAs discussed easily achieve this through use of strong dye-based chromophores, and the strength of absorption can be further tuned through the extent of overlap between HOMO and LUMO. The breadth of absorption is also important as a complementary absorption profile with the donor material is sought. For example, by replacement of the fluorene core of **3.1** with indacenodithiophene in **3.7**, the structure becomes more planar by the increased quinoidal character of the thiophene–phenyl bond. This extends the conjugation of the aromatic system, reducing the bandgap significantly to give an absorption profile that is more complementary to that of P3HT, the donor

polymer employed. In addition, the molar extinction coefficient of **3.7** benefits from the more delocalized LUMO, which has more spatial overlap with the HOMO relative to **3.1**. These factors result in an increased J_{SC} from 7.95 to 14.1 mA/cm^2 and an increase in PCE from 4.1% to 6.4% with P3HT as the donor.[45]

Second, the energy levels of the material must be optimized relative to the donor, with the EA of the acceptor designed to be as low as possible to maximize V_{OC} while maintaining efficient electron transfer. Given the high extinction coefficients of these acceptors as discussed, the offset between HOMO levels is equally important to optimize for these systems to ensure efficient hole transfer. Many calamitic NFAs are able to yield high V_{OC} values (0.8–1.2 V) through optimization of these energy levels, giving them a significant advantage over fullerene acceptors. It must be noted here that the lack of standardized measurement techniques between research groups for ionization potential and electron affinity determination makes it difficult to assess the effect of these properties in relative terms.

Third, the acceptor should ideally be designed to work with high performance polymers to achieve high efficiencies. Devices made with high mobility, low bandgap polymers such as the PTB7 derivatives are expected to result in higher efficiencies than those made with wide bandgap polymers such as P3HT, making it difficult to assess the relative potential of new acceptor materials.

Lastly, the aggregating nature of the acceptor is important in determining the morphology of the active layer. The material should crystallize enough that it forms some pure domains with an optimum charge percolation pathway and good charge transport properties but without forming large domains that limit the capacity for exciton splitting. Fused, planar systems such as indacenodithiophene can help promote crystallinity, as can the incorporation of polar groups such as cyano and imide functionalities, which facilitate self-organization through local dipole alignments. This can be balanced through the incorporation of bulky side chains such as branched 2-ethylhexyl or 4-hexylphenyl chains. Alternatively, the molecule is induced to adopt a twisted structure through the use of sterically clashing units such as the naphthalimide group used in **3.6**[50] or the BT−fluorene link in **3.1**.[40] In this way, crystallinity and solubility can be controlled while reducing the need for bulky nonabsorbing alkyl groups. In addition, twisted structures can provide more anisotropic charge transport similar to that of fullerenes and twisted perylene diimide structures, both of which show excellent charge transport properties.

CONCLUSIONS

It is clear that the research into non-fullerene acceptors for organic photovoltaics have progressed rapidly over recent years. Evaporated planar heterojunction devices have reached power conversion efficiencies of 8.4%,[33] while bulk heterojunction devices fabricated by solution processing have afforded PCEs of 6.8%.[46] The anticipated advantages of NFAs in terms of enhanced optical absorptivity and ease of frontier energy level engineering relative to fullerene acceptors have been clearly demonstrated in numerous studies. Judicious matching of the photoactive components' absorption profiles have afforded broad EQE responses and relatively high short-circuit currents with contributions from both channels I and II type charge generation. NFAs with lower electron affinities than the archetypical fullerenes have successfully been used in

conjunction with wide bandgap donors to enhance the open-circuit voltage. Similarly, NFAs with higher electron affinities are promising candidates in heterojunctions with narrow bandgap donors that are otherwise limited in performance by a small LUMO−LUMO offset. The understanding of dominant loss mechanisms is slowly emerging and so is the elucidation of structure−property relationships aimed at controlling the BHJ blend morphology and the morphological stability. With the continued strive for developing efficient NFAs and understanding the structure−property relationships, NFAs are bound to play an important role in the future development of organic photovoltaics.

AUTHOR INFORMATION

Corresponding Author

*E-mail: c.nielsen@imperial.ac.uk.

Notes

The authors declare no competing financial interest.

Biographies

Christian Nielsen obtained his Ph.D. in Chemistry from the University of Copenhagen in 2004. He is currently a research fellow and a project leader with research interests in organic electronics and bioelectronics.

Sarah Holliday obtained her M.Chem. from the University of Edinburgh and M.Res. in Plastic Electronics from Imperial College London. She is currently a Ph.D. student.

Hung-Yang Chen obtained his Ph.D. in Chemistry from National Taiwan University followed by a postdoctoral stay at Academia Sinica, Taiwan. He is currently a postdoctoral researcher.

Samuel Cryer obtained both his M.Sci. in Chemistry in 2011 and M.Res. in Plastic Electronics in 2013 from Imperial College London. He is currently a Ph.D. student.

Iain McCulloch is Professor of Polymer Materials in the Department of Chemistry at Imperial College London and Professor of Chemical Science at King Abdullah University of Science and Technology, with research interests in organic semiconducting materials synthesis, characterization, and devices. His achievements have been recognized with several awards including the Royal Society of Chemistry Tilden Prize for Advances in Chemistry and the Royal Society of Chemistry Creativity in Industry Prize, as well as a Royal Society Wolfson Merit Award.

ABBREVIATIONS

PBDTTT-C-T	poly[4,8-bis(5-(2-ethylhexyl)thiophen-2-yl)-benzo[1,2-b;4,5-b']dithiophene-2,6-diyl-alt-(4-(2-ethylhexanoyl)-thieno[3,4-b]thiophene-)-2-6-diyl)]
PBDTT-F-TT	poly[4,8-bis(5-(2-ethylhexyl)thiophen-2-yl)-benzo[1,2-b;4,5-b']dithiophene-2,6- 157 diyl-alt-(4-(2-ethylhexyl)-3-fluorothieno[3,4-b]-thiophene-)-2- 158 carboxylate-2−6-diyl)]
PDBT-T1	poly[dithieno[2,3-d:2',3'-d']benzo[1,2-b:4,5-b']dithiophene-co-1,3-bis(thiophen-2-yl)-benzo-[1,2-c:4,5-c']dithiophene-4,8-dione]

PBDTT-TT	poly[4,8-bis(5-(2- 171 ethylhexyl)thiophen-2-yl)benzo[1,2-*b*;4,5-*b'*]dithiophene-2,6- 172 diyl-*alt*-(4-(2-ethylhexyl)-3-fluorothieno[3,4-*b*]thiophene)-2- 173 carboxylate-2,6-diyl]
PffBT4T-2DT	poly[(5,6-difluoro-2,1,3-benzothiadiazol-4,7-diyl)-*alt*-(3,3'''-di(2-decyltetradecyl)-2,2';5',2'';5'',2'''-quaterthiophen-5,5'''-diyl)].
PBTI3T	poly[N-(2-hexyldodecyl)-2,2'-bithiophene-3,3'-dicarboximide-*alt*-5,5-(2,5-bis(3-decylthiophen-2-yl)-thiophene)].
PSEHTT	poly[(4,4'-bis(3-(2-ethylhexyl)dithieno[3,2-*b*:2',3'-*d*]silole)-2,6-diyl-*alt*-(2,5-bis(3-(2-ethylhexyl)thiophen-2yl)thiazolo[5,4-d]-thiazole)].
MEH-PPV	poly[2-methoxy-5-(2-ethylhexyloxy)-1,4-phenylenevinylene].
PTB7	poly[(4,8-bis-(2-ethylhexyloxy)-benzo(1,2-*b*:4,5-*b'*)dithiophene)-2,6-diyl-*alt*-(4-(2-ethylhexyl)-3-fluorothieno[3,4-b]thiophene-)-2-carboxylate-2-6-diyl)].

■ REFERENCES

(1) Liu, Y.; Zhao, J.; Li, Z.; Mu, C.; Ma, W.; Hu, H.; Jiang, K.; Lin, H.; Ade, H.; Yan, H. Aggregation and morphology control enables multiple cases of high-efficiency polymer solar cells. *Nat. Commun.* **2014**, *5*, 5293.

(2) Douglas, J. D.; Chen, M. S.; Niskala, J. R.; Lee, O. P.; Yiu, A. T.; Young, E. P.; Fréchet, J. M. J. Solution-Processed, Molecular Photovoltaics that Exploit Hole Transfer from Non-Fullerene, n-Type Materials. *Adv. Mater.* **2014**, *26*, 4313−4319.

(3) Fang, Y.; Pandey, A. K.; Nardes, A. M.; Kopidakis, N.; Burn, P. L.; Meredith, P. A Narrow Optical Gap Small Molecule Acceptor for Organic Solar Cells. *Adv. Energy Mater.* **2013**, *3*, 54−59.

(4) Li, C.; Wonneberger, H. Perylene imides for organic photovoltaics: yesterday, today, and tomorrow. *Adv. Mater.* **2012**, *24*, 613−636.

(5) Shivanna, R.; Shoaee, S.; Dimitrov, S.; Kandappa, S. K.; Rajaram, S.; Durrant, J. R.; Narayan, K. S. Charge generation and transport in efficient organic bulk heterojunction solar cells with a perylene acceptor. *Energy Environ. Sci.* **2014**, *7*, 435−441.

(6) Ye, L.; Sun, K.; Jiang, W.; Zhang, S.; Zhao, W.; Yao, H.; Wang, Z.; Hou, J. Enhanced Efficiency in Fullerene-Free Polymer Solar Cell by Incorporating Fine-designed Donor and Acceptor Materials. *ACS Appl. Mater. Interfaces* **2015**, *7*, 9274−9280.

(7) Jiang, W.; Ye, L.; Li, X.; Xiao, C.; Tan, F.; Zhao, W.; Hou, J.; Wang, Z. Bay-linked perylene bisimides as promising non-fullerene acceptors for organic solar cells. *Chem. Commun.* **2014**, *50*, 1024−1026.

(8) Zang, Y.; Li, C.-Z.; Chueh, C. C.; Williams, S. T.; Jiang, W.; Wang, Z.-H.; Yu, J.-S.; Jen, A. K. Y. Integrated Molecular, Interfacial, and Device Engineering towards High-Performance Non-Fullerene Based Organic Solar Cells. *Adv. Mater.* **2014**, *26*, 5708−5714.

(9) Sun, D.; Meng, D.; Cai, Y.; Fan, B.; Li, Y.; Jiang, W.; Huo, L.; Sun, Y.; Wang, Z. Non-Fullerene-Acceptor-Based Bulk-Heterojunction Organic Solar Cells with Efficiency over 7%. *J. Am. Chem. Soc.* **2015**, *137*, 11156−11162.

(10) Zhong, Y.; Trinh, M. T.; Chen, R.; Wang, W.; Khlyabich, P. P.; Kumar, B.; Xu, Q.; Nam, C.-Y.; Sfeir, M. Y.; Black, C.; Steigerwald, M. L.; Loo, Y.-L.; Xiao, S.; Ng, F.; Zhu, X. Y.; Nuckolls, C. Efficient Organic Solar Cells with Helical Perylene Diimide Electron Acceptors. *J. Am. Chem. Soc.* **2014**, *136*, 15215−15221.

(11) Zhang, X.; Lu, Z.; Ye, L.; Zhan, C.; Hou, J.; Zhang, S.; Jiang, B.; Zhao, Y.; Huang, J.; Zhang, S.; Liu, Y.; Shi, Q.; Liu, Y.; Yao, J. A Potential Perylene Diimide Dimer-Based Acceptor Material for Highly Efficient Solution-Processed Non-Fullerene Organic Solar Cells with 4.03% Efficiency. *Adv. Mater.* **2013**, *25*, 5791−5797.

(12) Zhang, X.; Zhan, C.; Yao, J. Non-Fullerene Organic Solar Cells with 6.1% Efficiency through Fine-Tuning Parameters of the Film-Forming Process. *Chem. Mater.* **2015**, *27*, 166−173.

(13) Liu, S.-Y.; Wu, C.-H.; Li, C.-Z.; Liu, S.-Q.; Wei, K.-H.; Chen, H.-Z.; Jen, A. K. Y. A Tetraperylene Diimides Based 3D Nonfullerene Acceptor for Efficient Organic Photovoltaics. *Adv. Sci.* **2015**, *2*, 1500014.

(14) Liu, Y.; Mu, C.; Jiang, K.; Zhao, J.; Li, Y.; Zhang, L.; Li, Z.; Lai, J. Y. L.; Hu, H.; Ma, T.; Hu, R.; Yu, D.; Huang, X.; Tang, B. Z.; Yan, H. A Tetraphenylethylene Core-Based 3D Structure Small Molecular Acceptor Enabling Efficient Non-Fullerene Organic Solar Cells. *Adv. Mater.* **2015**, *27*, 1015−1020.

(15) Liu, Y.; Lai, J. Y. L.; Chen, S.; Li, Y.; Jiang, K.; Zhao, J.; Li, Z.; Hu, H.; Ma, T.; Lin, H.; Liu, J.; Zhang, J.; Huang, F.; Yu, D.; Yan, H. Efficient non-fullerene polymer solar cells enabled by tetrahedron-shaped core based 3D-structure small-molecular electron acceptors. *J. Mater. Chem. A* **2015**, *3*, 13632−13636.

(16) Yan, Q.; Zhou, Y.; Zheng, Y.-Q.; Pei, J.; Zhao, D. Towards rational design of organic electron acceptors for photovoltaics: a study based on perylenediimide derivatives. *Chem. Sci.* **2013**, *4*, 4389−4394.

(17) Zhao, J.; Li, Y.; Lin, H.; Liu, Y.; Jiang, K.; Mu, C.; Ma, T.; Lin Lai, J. Y.; Hu, H.; Yu, D.; Yan, H. High-efficiency non-fullerene organic solar cells enabled by a difluorobenzothiadiazole-based donor polymer combined with a properly matched small molecule acceptor. *Energy Environ. Sci.* **2015**, *8*, 520−525.

(18) Margulies, E. A.; Shoer, L. E.; Eaton, S. W.; Wasielewski, M. R. Excimer formation in cofacial and slip-stacked perylene-3,4:9,10-bis(dicarboximide) dimers on a redox-inactive triptycene scaffold. *Phys. Chem. Chem. Phys.* **2014**, *16*, 23735−23742.

(19) Hartnett, P. E.; Timalsina, A.; Matte, H. S. S. R.; Zhou, N.; Guo, X.; Zhao, W.; Facchetti, A.; Chang, R. P. H.; Hersam, M. C.; Wasielewski, M. R.; Marks, T. J. Slip-stacked perylenediimides as an alternative strategy for high efficiency nonfullerene acceptors in organic photovoltaics. *J. Am. Chem. Soc.* **2014**, *136*, 16345−16356.

(20) Li, H.; Earmme, T.; Ren, G.; Saeki, A.; Yoshikawa, S.; Murari, N. M.; Subramaniyan, S.; Crane, M. J.; Seki, S.; Jenekhe, S. A. Beyond Fullerenes: Design of Nonfullerene Acceptors for Efficient Organic Photovoltaics. *J. Am. Chem. Soc.* **2014**, *136*, 14589−14597.

(21) Li, H.; Hwang, Y.-J.; Courtright, B. A. E.; Eberle, F. N.; Subramaniyan, S.; Jenekhe, S. A. Fine-Tuning the 3D Structure of Nonfullerene Electron Acceptors Toward High-Performance Polymer Solar Cells. *Adv. Mater.* **2015**, *27*, 3266−3272.

(22) Li, H.; Kim, F. S.; Ren, G.; Hollenbeck, E. C.; Subramaniyan, S.; Jenekhe, S. A. Tetraazabenzodifluoranthene diimides: building blocks for solution-processable n-type organic semiconductors. *Angew. Chem., Int. Ed.* **2013**, *52*, 5513−5517.

(23) Scott, L. T.; Hashemi, M. M.; Meyer, D. T.; Warren, H. B. Corannulene. A convenient new synthesis. *J. Am. Chem. Soc.* **1991**, *113*, 7082−7084.

(24) Amsharov, K. Y.; Jansen, M. C48 Buckybowl and C60 Fullerene Precursors on the Basis of Truxenone. *Z. Naturforsch., B: J. Chem. Sci.* **2007**, *62*, 1497−1508.

(25) Lu, R.-Q.; Xuan, W.; Zheng, Y.-Q.; Zhou, Y.-N.; Yan, X.-Y.; Dou, J.-H.; Chen, R.; Pei, J.; Weng, W.; Cao, X.-Y. A corannulene-based donor-acceptor polymer for organic field-effect transistors. *RSC Adv.* **2014**, *4*, 56749−56755.

(26) Lu, R.-Q.; Zhou, Y.-N.; Yan, X.-Y.; Shi, K.; Zheng, Y.-Q.; Luo, M.; Wang, X.-C.; Pei, J.; Xia, H.; Zoppi, L.; Baldridge, K. K.; Siegel, J. S.; Cao, X.-Y. Thiophene-fused bowl-shaped polycyclic aromatics with a dibenzo[a,g]corannulene core for organic field-effect transistors. *Chem. Commun.* **2015**, *51*, 1681−1684.

(27) Lu, R.-Q.; Zheng, Y.-Q.; Zhou, Y.-N.; Yan, X.-Y.; Lei, T.; Shi, K.; Zhou, Y.; Pei, J.; Zoppi, L.; Baldridge, K. K.; Siegel, J. S.; Cao, X.-Y. Corannulene derivatives as non-fullerene acceptors in solution-processed bulk heterojunction solar cells. *J. Mater. Chem. A* **2014**, *2*, 20515−20519.

(28) Nielsen, C. B.; Voroshazi, E.; Holliday, S.; Cnops, K.; Rand, B. P.; McCulloch, I. Efficient truxenone-based acceptors for organic photovoltaics. *J. Mater. Chem. A* **2013**, *1*, 73−76.

(29) Nielsen, C. B.; Voroshazi, E.; Holliday, S.; Cnops, K.; Cheyns, D.; McCulloch, I. Electron-deficient truxenone derivatives and their use in organic photovoltaics. *J. Mater. Chem. A* **2014**, *2*, 12348−12354.

(30) Pho, T. V.; Toma, F. M.; Chabinyc, M. L.; Wudl, F. Self-Assembling Decacyclene Triimides Prepared through a Regioselective Hextuple Friedel−Crafts Carbamylation. *Angew. Chem., Int. Ed.* **2013**, *52*, 1446−1451.

(31) Pho, T. V.; Toma, F. M.; Tremolet de Villers, B. J.; Wang, S.; Treat, N. D.; Eisenmenger, N. D.; Su, G. M.; Coffin, R. C.; Douglas, J. D.; Fréchet, J. M. J.; Bazan, G. C.; Wudl, F.; Chabinyc, M. L. Decacyclene Triimides: Paving the Road to Universal Non-Fullerene Acceptors for Organic Photovoltaics. *Adv. Energy Mater.* **2014**, *4*, 1301007.

(32) Chen, H.-Y.; Golder, J.; Yeh, S.-C.; Lin, C.-W.; Chen, C.-T.; Chen, C.-T. Diindeno[1,2-g:1′,2′-s]rubicene: all-carbon non-fullerene electron acceptor for efficient bulk-heterojunction organic solar cells with high open-circuit voltage. *RSC Adv.* **2015**, *5*, 3381−3385.

(33) Cnops, K.; Rand, B. P.; Cheyns, D.; Verreet, B.; Empl, M. A.; Heremans, P. 8.4% efficient fullerene-free organic solar cells exploiting long-range exciton energy transfer. *Nat. Commun.* **2014**, *5*, 3406.

(34) Verreet, B.; Cnops, K.; Cheyns, D.; Heremans, P.; Stesmans, A.; Zango, G.; Claessens, C. G.; Torres, T.; Rand, B. P. Decreased Recombination Through the Use of a Non-Fullerene Acceptor in a 6.4% Efficient Organic Planar Heterojunction Solar Cell. *Adv. Energy Mater.* **2014**, *4*, 1301413.

(35) Cnops, K.; Zango, G.; Genoe, J.; Heremans, P.; Martinez-Diaz, M. V.; Torres, T.; Cheyns, D. Energy Level Tuning of Non-Fullerene Acceptors in Organic Solar Cells. *J. Am. Chem. Soc.* **2015**, *137*, 8991−8997.

(36) Verreet, B.; Rand, B. P.; Cheyns, D.; Hadipour, A.; Aernouts, T.; Heremans, P.; Medina, A.; Claessens, C. G.; Torres, T. A 4% Efficient Organic Solar Cell Using a Fluorinated Fused Subphthalocyanine Dimer as an Electron Acceptor. *Adv. Energy Mater.* **2011**, *1*, 565−568.

(37) Ebenhoch, B.; Prasetya, N. B. A.; Rotello, V. M.; Cooke, G.; Samuel, I. D. W. Solution-processed boron subphthalocyanine derivatives as acceptors for organic bulk-heterojunction solar cells. *J. Mater. Chem. A* **2015**, *3*, 7345−7352.

(38) Winzenberg, K. N.; Kemppinen, P.; Scholes, F. H.; Collis, G. E.; Shu, Y.; Birendra Singh, T.; Bilic, A.; Forsyth, C. M.; Watkins, S. E. Indan-1,3-dione electron-acceptor small molecules for solution-processable solar cells: a structure-property correlation. *Chem. Commun.* **2013**, *49*, 6307−6309.

(39) Shi, H.; Fu, W.; Shi, M.; Ling, J.; Chen, H. A solution-processable bipolar diketopyrrolopyrrole molecule used as both electron donor and acceptor for efficient organic solar cells. *J. Mater. Chem. A* **2015**, *3*, 1902−1905.

(40) Holliday, S.; Ashraf, R. S.; Nielsen, C. B.; Kirkus, M.; Röhr, J. A.; Tan, C.-H.; Collado-Fregoso, E.; Knall, A.-C.; Durrant, J. R.; Nelson, J.; McCulloch, I. A Rhodanine Flanked Nonfullerene Acceptor for Solution-Processed Organic Photovoltaics. *J. Am. Chem. Soc.* **2015**, *137*, 898−904.

(41) Lin, Y.; Li, Y.; Zhan, X. A Solution-Processable Electron Acceptor Based on Dibenzosilole and Diketopyrrolopyrrole for Organic Solar Cells. *Adv. Energy Mater.* **2013**, *3*, 724−728.

(42) Fang, Y.; Pandey, A. K.; Lyons, D. M.; Shaw, P. E.; Watkins, S. E.; Burn, P. L.; Lo, S.-C.; Meredith, P. Tuning the Optoelectronic Properties of Nonfullerene Electron Acceptors. *ChemPhysChem* **2015**, *16*, 1295−1304.

(43) Bai, H.; Wang, Y.; Cheng, P.; Wang, J.; Wu, Y.; Hou, J.; Zhan, X. An electron acceptor based on indacenodithiophene and 1,1-dicyanomethylene-3-indanone for fullerene-free organic solar cells. *J. Mater. Chem. A* **2015**, *3*, 1910−1914.

(44) Lin, Y.; Zhang, Z.-G.; Bai, H.; Wang, J.; Yao, Y.; Li, Y.; Zhu, D.; Zhan, X. High-performance fullerene-free polymer solar cells with 6.31% efficiency. *Energy Environ. Sci.* **2015**, *8*, 610−616.

(45) Holliday, S.; Ashraf, R. S.; Wadsworth, A.; Baran, D.; Nielsen, C. B.; Yousaf, A.; Tan, C.-H.; Dimitrov, S. D.; Shang, Z.; Gasparini, N.; Brabec, C. J.; Salleo, A.; Durrant, J. R.; McCulloch, I. High Efficiency P3HT Based Polymer Solar Cells with a New Small Molecule Acceptor. 2015, Submitted.

(46) Lin, Y.; Wang, J.; Zhang, Z.-G.; Bai, H.; Li, Y.; Zhu, D.; Zhan, X. An Electron Acceptor Challenging Fullerenes for Efficient Polymer Solar Cells. *Adv. Mater.* **2015**, *27*, 1170−1174.

(47) Bloking, J. T.; Han, X.; Higgs, A. T.; Kastrop, J. P.; Pandey, L.; Norton, J. E.; Risko, C.; Chen, C. E.; Brédas, J.-L.; McGehee, M. D.; Sellinger, A. Solution-Processed Organic Solar Cells with Power Conversion Efficiencies of 2.5% using Benzothiadiazole/Imide-Based Acceptors. *Chem. Mater.* **2011**, *23*, 5484−5490.

(48) Zhou, Y.; Dai, Y.-Z.; Zheng, Y.-Q.; Wang, X.-Y.; Wang, J.-Y.; Pei, J. Non-fullerene acceptors containing fluoranthene-fused imides for solution-processed inverted organic solar cells. *Chem. Commun.* **2013**, *49*, 5802−5804.

(49) Graham, K. R.; Cabanetos, C.; Jahnke, J. P.; Idso, M. N.; El Labban, A.; Ngongang Ndjawa, G. O.; Heumueller, T.; Vandewal, K.; Salleo, A.; Chmelka, B. F.; Amassian, A.; Beaujuge, P. M.; McGehee, M. D. Importance of the Donor:Fullerene Intermolecular Arrangement for High-Efficiency Organic Photovoltaics. *J. Am. Chem. Soc.* **2014**, *136*, 9608−9618.

(50) Kwon, O. K.; Park, J.-H.; Kim, D. W.; Park, S. K.; Park, S. Y. An All-Small-Molecule Organic Solar Cell with High Efficiency Non-fullerene Acceptor. *Adv. Mater.* **2015**, *27*, 1951−1956.

(51) Kim, Y.; Song, C. E.; Moon, S.-J.; Lim, E. Rhodanine dye-based small molecule acceptors for organic photovoltaic cells. *Chem. Commun.* **2014**, *50*, 8235−8238.